I.A.U
Karaj branch

Journal of
A p p l ied
C hemical
R esearch
jacr.kiau.ac.ir

Journal of Applied Chemical Research, 11, 3, 19-27 (2017)

Green Synthesis of α-Fe_2O_3 (hematite) Nanoparticles using *Tragacanth* Gel

Saeid Taghavi Fardood[1], Ali Ramazani*[1], Zahra Golfar[1], Sang Woo Joo*[2]

[1]*Department of Chemistry, University of Zanjan, Zanjan, Iran*

[2]*School of Mechanical Engineering, Yeungnam University, Gyeongsan, Republic of Korea*

(Received 08 Dec. 2016; Final version received 06 Mar. 2017)

Abstract

α-Fe_2O_3 (hematite) nanoparticles were synthesized using tragacanth gel as biotemplate and iron chloride as the iron source by the sol-gel method. This method has many advantages such as nontoxic, economic viability, ease to scale up, less time consuming and environmental friendly approach for the synthesis of α-Fe_2O_3 nanoparticles without using any organic chemicals. Nanoparticles were characterized by Fourier transform infrared (FT-IR) spectroscopy, UV-visible spectroscopy and X-ray diffraction (XRD). The powder X-ray diffraction (XRD) analysis revealed the formation of Rhombohedral phase α-Fe_2O_3 with average particle size of 21 nm.

Keywords: *α-Fe_2O_3, Tragacanth gel, Nanobiotechnology, natural Hydrogel, Sol-gel.*

[*]***Corresponding author:*** *Ali Ramazani, Department of Chemistry, University of Zanjan, P O Box 45195-313, Zanjan, Iran. E-mail: aliramazani@gmail.com*, Phone: 00982433052572, Fax: 00982433052477.
Sang Woo Joo' School of Mechanical Engineering, Yeungnam University, Gyeongsan 712-749, Republic of Korea. E-mail: swjoo@yu.ac.kr. Phone: +82 53 810 1456, *Fax*: +82 53 810 2062.

Introduction

Recently, nanomaterials nanoparticles have received more attention due to their physical properties and technological applications. Nanoparticles of iron oxide, in its different phases, are being currently explored for their diverse range of applications such as magnetic storage media, environment protection, sensors, catalysis, clinical diagnosis and treatment [1-7].

Fe_2O_3 has four phases: α-Fe_2O_3 (hematite), β-Fe_2O_3, γ-Fe2O3 (maghemite), and ξ-Fe2O3 [8]. Among them α-Fe_2O_3 has the corundum structure, while the others have the cubic structure [9]. Gamma and epsilon type Fe_2O_3 are ferromagnetic; alpha Fe_2O_3 is a canted antiferromagnetic while beta type Fe_2O_3 is a paramagnetic material. As alpha Fe_2O_3 has canted magnetism which means that the magnetic moments of the two magnetic sub-lattices do not fully cancel each other and result in small magnetic moment value in the direction of the basal plane.

When the size of the magnetic particles becomes very small the magnetic moment in the domain fluctuates in direction, due to thermal agitation which leads to superparamagnetism. Among different magnetic nanoparticles, α- Fe_2O_3 is of great interest for potential applications as a gas sensor, lithium ion battery, catalyst, and pigment [10-12]. The environmental friendly α Fe_2O_3 (hematite), an n-type semiconductor is the most stable iron oxide phase under ambient conditions. It can be used as gas sensors, catalysts, high density magnetic recording media, clinical therapy and diagnosis, negative temperature coefficient of resistance, ferrofluids, high resistivity to corrosion, printing ink, magnetic resonance imaging, photoelectrodes for solar energy conversion and especially biomedical field [13-20]. There are many developed methods for the synthesis of Iron oxide such as: sol-gel [21], electrochemical techniques [22], sputtering [23], vapor deposition [24] and hydrothermal [25]. The mentioned methods have proven to be advantageous in different aspects, but recently attentions have drawn to methods which are both eco-friendly and commercially feasible.

Tragacanth gum (TG) is a naturally occurring complex, acidic polysaccharide derived as an exudate from the bark of Astragalus gummifer (Fabaceae family), a native tree of western Asia. It is commercially produced mostly in Iran and Turkey [26]. This biopolymer is an arabinogalactan type of natural gum and its structural, physicochemical, compositional, solution, thermal, rheological and emulsifying properties have been well characterized and studied [27, 28]. This natural polymer consists of a mixture of water-soluble (tragacanthin) and water-swellable (bassorin) polysaccharide fractions [26,29].

α-Fe_2O_3 (hematite) is the most stable iron oxide under ambient conditions. This transition metal oxide has been extensively investigated because it has unique electrical and catalytic properties [9]. In the present work, for the first time, we have synthesized ferric oxide nanoparticles using TG by the sol-gel method as a cheap and friendly approach to the nature. The samples were characterized by X-ray diffraction (XRD), Fourier transform infrared spectroscopy (FTIR), UV-Vis spectroscopy.

Experimental

Material and methods

The Tragacanth gum (TG) was obtained from a local health food store. Iron Chloride $FeCl_3$ was purchased from merck (Darmstadt, Germany) and used without further purification. The IR spectra were measured on a Jasco 6300 FT-IR spectrometer (KBr disks). UV-Vis absorption spectra were prepared on a Metrohm (Analytical Jena-Specord 205) double beam instrument. The measurement was carried out from 200 nm to 700 nm wavelength for all of the samples. The structural properties of synthesized nanoparticles were investigated by X-ray powder diffraction (XRD) pattern on a X'Pert-PRO advanced diffractometer using Cu (Kα) radiation (wavelength: 1.5406 Å) at 40 kV and 40 mA at room temperature in the range of 2θ from 20 to 80º.

Synthesis of α-Fe_2O_3 nanoparticles using Tragacanth gum

In a typical synthesis, 1 mmole of $FeCl_3$ was dissolved in 5 ml of distilled water and then stirred for 5 min. Meanwhile, 0.2 g of the Tragacanth gum (TG) was dissolved in 40 ml of distilled water and stirred for 80 min at 70 ºC to achieve a clear Tragacanth gel (TG) solution. After that, the $FeCl_3$ solution was added to the TG solution, and the container was placed in a sand bath. The temperature of the sand bath was fixed at 70 ºC and stirring was continued for 12 h to obtain a black colour resin. The final product was calcined at 600 ºC temperatures in air for 3h to obtain a black powder of α-Fe_2O_3.

Results and discussion

Preparation of α-Fe_2O_3 nanoparticles.

Synthesis of α-Fe_2O_3-NPs was reported *via* various methods such as sol-gel [30], emulsion precipitation [31], microwave irradiation [32-33], hydrothermal [34] and co-precipitation [35]. In this study, we demonstrated a new method of sol-gel to synthesize α-Fe_2O_3-NPs using Tragacanth gum (TG) without using any organic chemicals. The major advantages of this

research is the synthesis of α-Fe_2O_3-NPs in eco-friendly, very cost effective and green conditions. Particle sizes of the synthesized α-Fe_2O_3-NPs by various methods are listed in Table1. The presented results show that using of Tragacanth gum-based Sol-gel method leads to the formation of smaller particle sizes for the prepared α-Fe_2O_3-NPs.

Table1. Particle sizes of the synthesized α-Fe_2O_3-NPs by various methods.

Entry	method	Size of nanoparticles*	Ref.
1	Sol-Gel	22-56 nm	[30]
2	emulsion precipitation	42 nm	[31]
3	microwave	57 nm	[32]
	microwave	68-79 nm	[33]
4	hydrothermal	40-50 nm	[34]
5	co-precipitation	30 nm	[35]
6	Sol-gel (TG)	21nm	This work

*Calculated by Scherer formula

Characterization of α-Fe_2O_3 nanoparticles.

FTIR spectra were recorded in solid phase using the KBr pellet technique in the range of 400-4000 cm^{-1}. FTIR The formation of α-Fe_2O_3 nanoparticles was further confirmed by FT-IR spectroscopy in Figure 1. The spectra show two characteristic bands at 437-440 cm^{-1} and 537–541 cm^{-1} which corresponds to Fe-O stretching. The highest one ν_1 (Figure 1) observed at 539 cm^{-1} corresponds to intrinsic stretching vibration of the, Fe↔O, where as the ν_2-lowest band, usually observed at 439 cm^{-1}, is assigned to bending vibration of the, O↔Fe↔O [36].

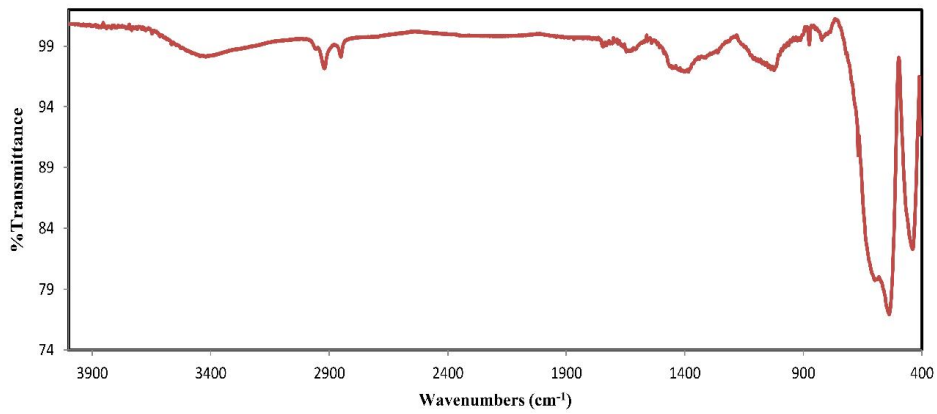

Figure 1. FT-IR spectrum of α-Fe_2O_3 NPs.

The room temperature UV-Vis absorption spectrum of the α-Fe2O3 is shown in Figure 2.

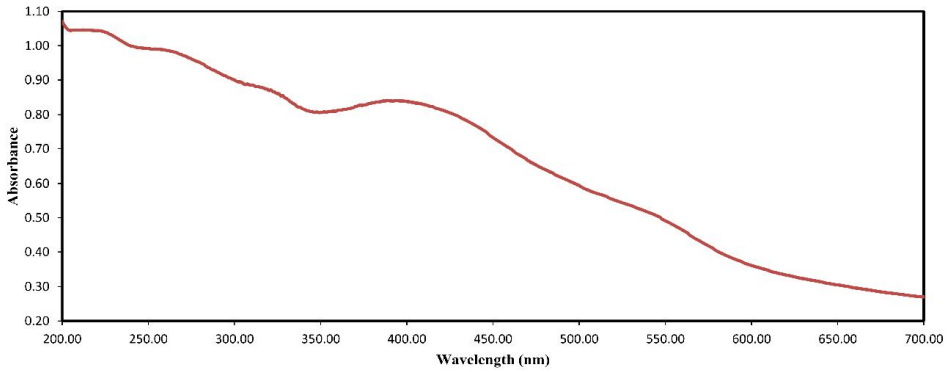

Figure 2. UV-Vis spectrum of α-Fe_2O_3 NPs.

UV-vis absorption measurement of the as-prepared α-Fe_2O_3 nanoparticles were carried out. According to the literature [37,38], two absorption regions are expected between 200 nm and 600 nm. The absorptions were observed at 200–300 nm centered at 262 nm (region 1) and at 400–600 nm with maximum about 533 nm (region 2) in Fig. 2. The first region mainly results from the ligand to metal charge transfer transitions and partly contributed from the Fe^{3+} ligand field transitions $^6A_1 \rightarrow {}^4T_1$ (^4P). In the second region the absorption peaks are mainly due to the $^6A_1 + {}^6A_1 \rightarrow {}^4T_1$ (^4G)+ $^4T_1$ (^4G) excitation of an Fe^{3+}- Fe^{3+} pair, possibly overlapped with the contributions of $^6A_1 \rightarrow {}^4E$, $^4A_1$ (^4G) ligand field transition and the charge-transfer band tail [39].

Similar results were reported for the preparation of α-Fe_2O_3 nanoparticles by oxygenating of pure iron. The absorption bands (α-Fe_2O_3 nanoparticles suspended in ethanol) at 310 and414 nm are assigned to the $^6A_1{}^4T_1$ (^4P) and $^6A_1{}^4T_2$ while the absorption bands in the visible region near 580 nm and 681 nm are assigned to the $^6A_1 + {}^6A_1$ $^4T_1$ (^4G) + $^4T_1$ (^4G) double excitation process (DEP) and $^6A_1{}^4T_2$ (^4G) ligand field transitions of Fe^{3+} respectively [40]. The crystal structure confirmation analysis was carried out by the X-ray diffraction patterns. XRD patterns of the product obtained by calcination of precursor at 600 °C are shown in Figure 3.

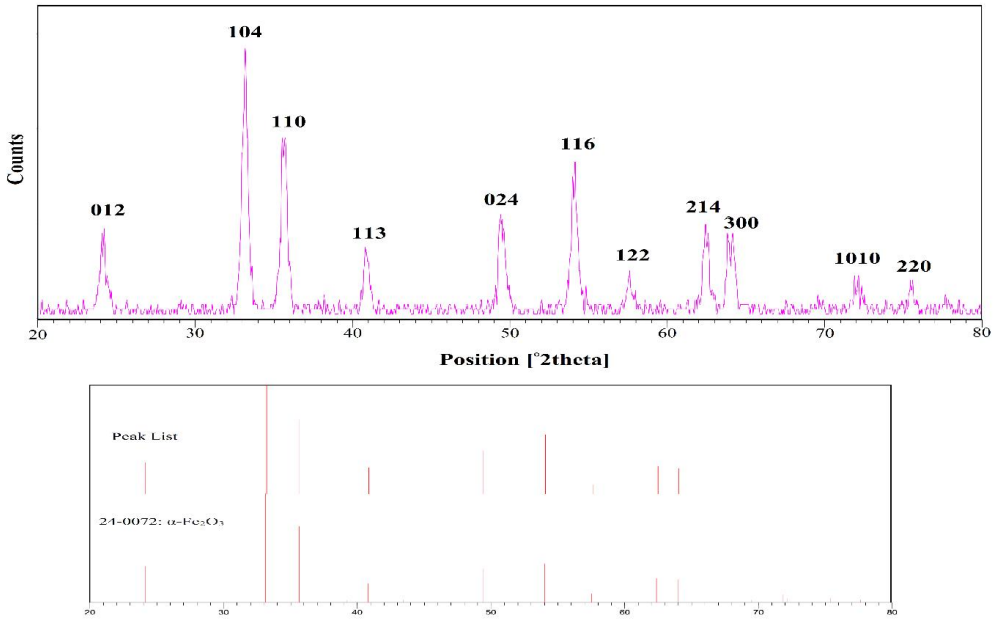

Figure 3. XRD pattern of synthesized α-Fe_2O_3 NPs.

XRD analysis showed a series of diffraction peaks at 2θ of 24.12, 33.17, 35.65, 40.87, 49.46, 54.07, 57.61 ,62.46, 64.03, 72.03 and 75.55 can be assigned to (012), (104), (110), (113), (024), (116), (122), (214), (300), (1010) and (220) planes, respectively. All the diffraction peaks were readily indexed to a pure rhombohedral phase of α-Fe_2O_3 (JSPDS Card no. 24-0072) with a=b = 5.0380 Å and c = 13.7720 Å. The diffraction patterns are well matched with the literature [41] and no impurity peaks were observed.

Furthermore, the strong and sharp diffraction peaks confirm the high crystallinity of the products. The average particle size of α-Fe_2O_3 nanoparticles was determined from the full width at half maximum (FWHM) of the XRD patterns using the well- known Scherer formula: $D = 0.9\lambda/\beta\cos\theta$ where D is the crystallite size (nm), β is the full width at half maximum of the peak, λ is the X-ray wavelength of Cu Kα= 0.154 nm and θ is the Bragg aangle [42]. Using the above method we obtained an average size of 21 nm for α-Fe_2O_3 nanoparticles.

Conclusion

In this paper, we have reported for the first time, the green synthesis of α-Fe_2O_3 nanoparticles that was carried out by the sol-gel method in Tragacanth gel (TG) as a bio-polymeric template. A pure hematite α-Fe_2O_3 phase was formed after heat treatment at 600 °C for only 3 h. This method has many advantages such as non toxic, economic viability, ease to scale up,

less time consuming and environmental friendly approach for the synthesis of α-Fe_2O_3 nanoparticles without using any organic chemicals.

Acknowledgment

This work was supported by the *Iran National Science Foundation: INSF* and the University of Zanjan.

References

[1] F. Sadri, A. Ramazani, A. Massoudi, M. Khoobi, R. Tarasi, A. Shafiee, V. Azizkhani, L. Dolatyari, S. W. Joo, *Green Chem. Lett. Rev.,* 7, 257(2014).

[2] E. Mirhadi, A. Ramazani, M. Rouhani, S. W. Joo, *Chemija*., 24, 320(2013).

[3] T. Ohmori, H. Takahashi, H. Mametsuka, E. Suzuki, *Phys. Chem. Chem. Phys.,* 2, 3519 (2000).

[4] L. H. Huo, W. Li, L. H. Lu, H. N. Cui, S. Q. Xi, J. Wang, B. Zhao, Y. C. Shen, Z. H. Lu, *Chem. Mater*., 12, 790(2000)

[5] A. Ramazani, M. Rouhani, S. W. Joo, *Adv. Mater. Res*., 875-877, 202(2014).

[6] Z. Y. Sun, H. Q. Yuan, Z. M. Liu, B. X. Han, X. R. Zhang, *Adv. Mater.*, 17 2993 (2005).

[7] J. Chen, L. N. Xu, W. Y. Li, X. L. Gou, , *Adv. Mater.*, 17, 582 (2005).

[8] R. M. Cornell, U. Schwertmann, The Iron Oxide, VCH, Weinheim, Germany (1996).

[9] M. V. Kovalenko, M. I. Bodnarchuk, R. T. Lechner, G. Hesser, F. Schaffler, W. Heiss, *J. Am. Chem. Soc.,* 129, 6352 (2007).

[10] N. Mimura, L. Takahara; M. Saito, T. Hattori, K. Ohkuma, M. Ando, *Catal. Today*., 45, 61 (1998).

[11] Y. R. Uhm, W. W. Kim, C. K. Rhee, *Scripta Mater.,* 50 561 (2004).

[12] H. K. Edwards, E. Evans, S. McCaldin, P. Blood, D. H. Gregory, M. Poliakoff, *J. Phys. Conference Series*, 26, 195 (2006).

[13] S. W. Cao, Y. J. Zhu, *J. Phys. Chem. C.,* 112, 6253 (2008).

[14] A. Kong, H. W. Wang, J. Li, Y. K. Shan, *Mater. Lett.,* 62, 943 (2008).

[15] V. Kesavan, P. S. S. Sivanand, S. Chandrasekaran, Yu. Koltypin, A. Gedanken, *Angew. Chem. Int. Ed.,* 38, 3521 (1999).

[16] L. H. Huo, W. Li, L. H. Lu, H. N. Cui, S. Q. Xi, J. Wang, B. Zhao, Y. C. Shen, Z. H. Lu, *Chem. Mater.* 12, 790 (2000).

[17] K. Suresh, K. C. Patil, *J. Mater. Sci. Lett*., 12, 572 (1993).

[18] M. Kroell, M. Pridoehl, G. Zimmermann, L. Pop, S. Odenbach, A. Hartwig, *J. Magn. Magn. Mater*., 289, 21(2005).

[19] Y. S. Kang, S. Risbud, J. F. Rabolt, P. Stroeve, *Chem. Mater.* 8, 2209(1996).

[20] S. Zhang, X. J. Chen, C. R. Gu, Y. Zhang, J. D. Xu, Z. P. Bian, D. Yang, N. Gu, 4, 70(2009).

[21] M. Niederberger, *Acc. Chem. Res*., 40, 793(2007).

[22] D. Ramimoghadam, S. Bagheri, S. B. A. Hamid, *J. Magn. Magn. Mater.,* 368, 207(2014).

[23] E. L. Miller, D. Paluselli, B. Marsen, R. E. Rocheleau, *Thin Solid Films.*, 466, 307(2004).

[24] S. Park, S. Lim, H. Choi,. *Chem. Mater*., 18, 5150(2006).

[25] J. Ma, J. Lian, X. Duan, X. Liu, W. Zheng, *J. Phys. Chem. C*., 114, 10671(2010).

[26] G. O. Phillips, P. A. Williams, Handbook of Hydrocolloids, Woodhead Publishing Limited, Cambridge (2009).

[27] M. J. Zohuriaan, F. Shokrolahi, *Polym. Test.,* 23, 575(2004).

[28] F. Chenlo, R. Moreira, C. Silva, *J. Food Eng.,* 96, 107(2010).

[29] N. Gralen, M. Karrholm, *J. Coll. Sci*., 5, 21(1950).

[30] S. Akbar, S. Hasanain, N. Azmat and M. Nadeem, (2004), arXiv preprint cond-mat/0408480.

[31] S. K. Sahoo, K. Agarwal, A. K. Singh, B. G. Polke and K. C. Raha, *Int. J. Eng. Sci. Technol.,* 2, 118(2010).

[32] S. Mohammadi, M. Khorasani-Motlagh, S. Jahani, M. Yousefi, *Int. J. Nanosci. Nanotechnol.,* 8, 87(2012).

[33] Y. Huang, D. Ding, M. Zhu, W. Meng, Y. Huang, F. Geng, J. Li, J. Lin, C. Tang and Z. Lei, *Sci. Technol. Adv. Mater.,* 16, 014801(2015).

[34] M. Mohammadikish, *Ceram. Int*., 40, 1351(2014).

[35] M. Farahmandjou, F. Soflaee, *Phys. Chem. Res.,* 3, 193(2015).

[36] B. Zhao, Y. Wang, H. Guo, J. Wang, Y. He. Z. Jiao, M. Wu., *Mater. Sci. Poland.,* 25, 1143(2007).

[37] B. S. Zou, W. Huang, M. Y. Han, S. F. Y. Li, X. C. Wu, Y. Zhang, J. Zhang, J. S. Zhang, P. F. Wu, R. Y. Wang, *J. Phys. Chem. Solids*., 58, 1315(1997).

[38] Y. P. He, Y. M. Miao, C. R. Li, S. Q. Wang, L. Cao, S. S. Xie, G. Z. Yang, B. S. Zou, C. Burda, *Phys. Rev. B.,* 71, 125411(2005).

[39] Y. Y. Xu, D. Zhao, X. J. Zhang, W. T. Jin, P. Kashkarov, H. Zhang, *Physica E*., 41

806(2009).

[40] G. Zhang, Y. Xu, D. Gao, Y. Sun, *J. Alloy. Compd.,* 509, 885(2011).

[41] J. Hua, J. Gengsheng, *Mater. Lett.,* 63, 2725 (2009).

[42] H. P. Klug, L. E. Alexander, X-ray Diffraction Procedures for Polycrystalline and Amorphous Materials, Wiley, New York (1974).